NASA CONTRACTOR REPORT

NASA CR-970

A STUDY OF AN ELECTRIC FIELD MEASURING INSTRUMENT

by S. H. Levine and S. R. Harrison

Prepared by
NORTHROP CORPORATE LABORATORIES
Hawthorne, Calif.
for Ames Research Center

NATIONAL AERONAUTICS AND SPACE ADMINISTRATION • WASHINGTON, D. C. • JUNE 1968

NASA CR-970

A STUDY OF AN ELECTRIC FIELD MEASURING INSTRUMENT

By S. H. Levine and S. R. Harrison

Issued by Originator as Report No. NCL 67-39

Prepared under Contract No. NAS 2-4143, Phase I and Phase II, by
NORTHROP CORPORATE LABORTORIES
Hawthorne, Calif.

for Ames Research Center

NATIONAL AERONAUTICS AND SPACE ADMINISTRATION

For sale by the Clearinghouse for Federal Scientific and Technical Information
Springfield, Virginia 22151 – CFSTI price $3.00

FOREWORD

This study was conducted by Northrop Corporate Laboratories, Hawthorne, California, in accordance with contract NAS2-4143, "A Study of an Electric Field Measuring Instrument," covering Phase I and Phase II of a program to build a flight model of the cesium ion beam electric field meter. This report is the final engineering report for these two phases and has been assigned NCL 67-39 as a company report number. Dr. William I. Linlor, Chief, Electrodynamics Branch, NASA/Ames Research Center was the Contract Monitor.

ABSTRACT

The feasibility of employing a cesium ion beam electric field meter has been experimentally investigated in the laboratory using two types of cesium ion sources. The first source used radiant heating, the other electron bombardment heating. Excellent results were obtained with these sources attaining a sensitivity for measuring electric fields of 0.03 volts/meter. Methods for attaining sensitivities of the order of 0.01 V/m are presented together with a preliminary theoretical investigation of the processes pertaining to the production of cesium ions in the ionizer. Also, an electronic-readout system design is presented so that all aspects of constructing a cesium ion beam electric field instrument have been studied.

TABLE OF CONTENTS

SECTION 1.0

INTRODUCTION

Traditionally, electric field measuring devices that have been used to determine the electric field in the atmosphere,[1,2,3] the stratosphere,[4] or the ionosphere[5] utilize the field machine, the potential probe, or some modification of these devices. In general, these instruments have very low sensitivity. Palmer[6] describes a vibrating disc-type field mill particularly suited for spacecraft measurements designed to measure the magnitude and direction of the electric fields from 1300 Volts/meter to 1,300,000 V/m. Gdalevich[5] has flown an electric field meter on rockets into the ionosphere reporting measured values of approximately 50 V/m to several hundred V/m. The sensitivity threshold of his instrument was 6 V/m with a maximum measuring error of 40 V/m; however, the electric fields at the surface of the rockets in their experiments were determined to be larger than the ambient electric field by a factor of 100. Thus, electric fields of the order of 10^{-1} V/m are reported to exist in the ionosphere. Cole and Sellen[7] report using an electron emissive type E-meter to successfully measure the electric field on a spacecraft during the Ion Engine Ballistic Flight Tests of the Air Force Project 661A Series in 1964. This emissive E-meter determines the electric field by its effect on electron trajectories. The design of Cole and Sellen is reported to measure on its most sensitive scale a field strength of 100 V/m to within 10 V/m.

In space[8] it is desirous to measure fields as small as 10^{-3} V/m to 10^{-6} V/m, although potentials induced on the vehicle due to photo-electric electrons, impinging plasmas, etc., will beset the experimentor with major difficulties. It will, nevertheless, be necessary to construct an electric field measuring instrument with greater sensitivity than has been reported to date.

Low energy charged particles are easily deflected by small electric fields and, thus, satisfy the requirement of high sensitivity. A study was conducted under NASA contract NAS2-2895, "Feasibility of Using Radioactive Sources to Measure Electric Field Intensity in Space," to determine the applicability of using this method for space applications including the use of radioactive sources to supply heat[9]. Both electron beams and heavy ions were considered since, for the same energy, they are equally deflected by electric fields. However, electrons are orders of magnitude more sensitive to magnetic fields than heavy ions, and for space this effect must be minimized. This fact, together with the recent advances made in cesium ion engines for electrical space propulsion, caused us to place greater emphasis on a cesium beam deflection type instrument. The study showed that a cesium beam device offered great advantages including greater sensitivity for measuring an electric field in space. Consequently, a program was initiated under NASA contract NAS2-4143 to test this premise in the laboratory. This report describes the Phase I and Phase II effort performed under this contract; however, for completeness, a brief summary of the theory of the cesium ion beam electric field instrument is presented in the first part of Section II. The latter part of Section II considers the conditions for emission of cesium ions from the ionizer channel.

Two cesium ion beam sources (one radiant heated and the second heated by electron bombardment) have been designed, fabricated, and tested. The design and fabrication of these instruments are described in Section III. The successful operation of these sources, together with the experimental data and analysis, are given in Section IV. Pertinent facts on these investigations are summarized and a discussion on the potential of this device for measuring small electrical fields in space are given in the last section of this report. Included in this discussion is a design of an electronic system for reading out the data.

SECTION 2.0

THEORY OF OPERATION

2.1 CHARGED PARTICLE MOTION IN THE ELECTRIC AND MAGNETIC FIELD

When a charged particle moves in electric and magnetic fields, it is acted upon by a force given by the Lorentz equation.

$$\underline{F} = q\,(\underline{E} + \dot{\underline{r}} \times \underline{B}) = m\,\ddot{\underline{r}} \qquad (1)$$

where

$\underline{F}$ = force vector
q = particle charge
$\underline{E}$ = electric field vector
$\underline{r}$ = position vector of the charged particle
$\underline{B}$ = magnetic induction
m = particle mass

Equation (1) has been solved under the following assumptions:

(1) the electric and magnetic fields acting on the charged particle are uniform over the volume through which the particle moves;

(2) the electric and magnetic fields are constant or slowly varying in time.

These assumptions are not very restrictive, consequently, the general solution provides a realistic set of equations for studying means of measuring the electric field in space.

Studies have been performed under a NASA/Ames contract No. NAS2-2895-2, using the general solution. The study considers devices with and without large local magnetic fields. In the analysis, a beam of charged particles is placed in a coordinate system as shown in Figure 1. Positioning the beam in the x direction and assuming a transit time, T, small compared to the period of the cyclotron resonance frequency, i.e.,

$$T \ll \frac{2\pi}{(q/m)\,|B|} \tag{2}$$

$$x(T) = L = \tfrac{1}{2}\,(q/m)\,E_x\,T^2 + V_x\,T \tag{3a}$$

$$y(T) = D_y = \tfrac{1}{2}\,(q/m)\,(E_y - B_z\,V_x)\,T^2 \tag{3b}$$

$$z(T) = D_z = \tfrac{1}{2}\,(q/m)\,(E_z + B_y\,V_x)\,T^2 \tag{3c}$$

where L is the distance between source and detector and D_y and D_z are the deflections in the y and z directions.

The E_z component of the electric field can be made dominant by placing the beam close to the surface of the vehicle. From equation (3c), it follows that the magnetic field will contribute significantly to the deflection, D_z, unless

$$|B| \ll \left|\frac{E_z}{V_x}\right| = \frac{|E_z|}{[2\,(q/m)\,v_o]^{\frac{1}{2}}} \tag{4}$$

When the magnetic field is sufficiently low that the inequality given in equation (4) holds, the deflection in the z direction is given by equation (5) where $q\,v_o$ is the potential energy of the ions.

$$D = D_z = \left|\frac{E_z\,L^2}{4\,v_o}\right| \tag{5}$$

A beam deflection device for measuring the electric field in space can be optimized against the effect of the magnetic field by using a low energy beam of heavy ions. Low energy, because from equation (5),

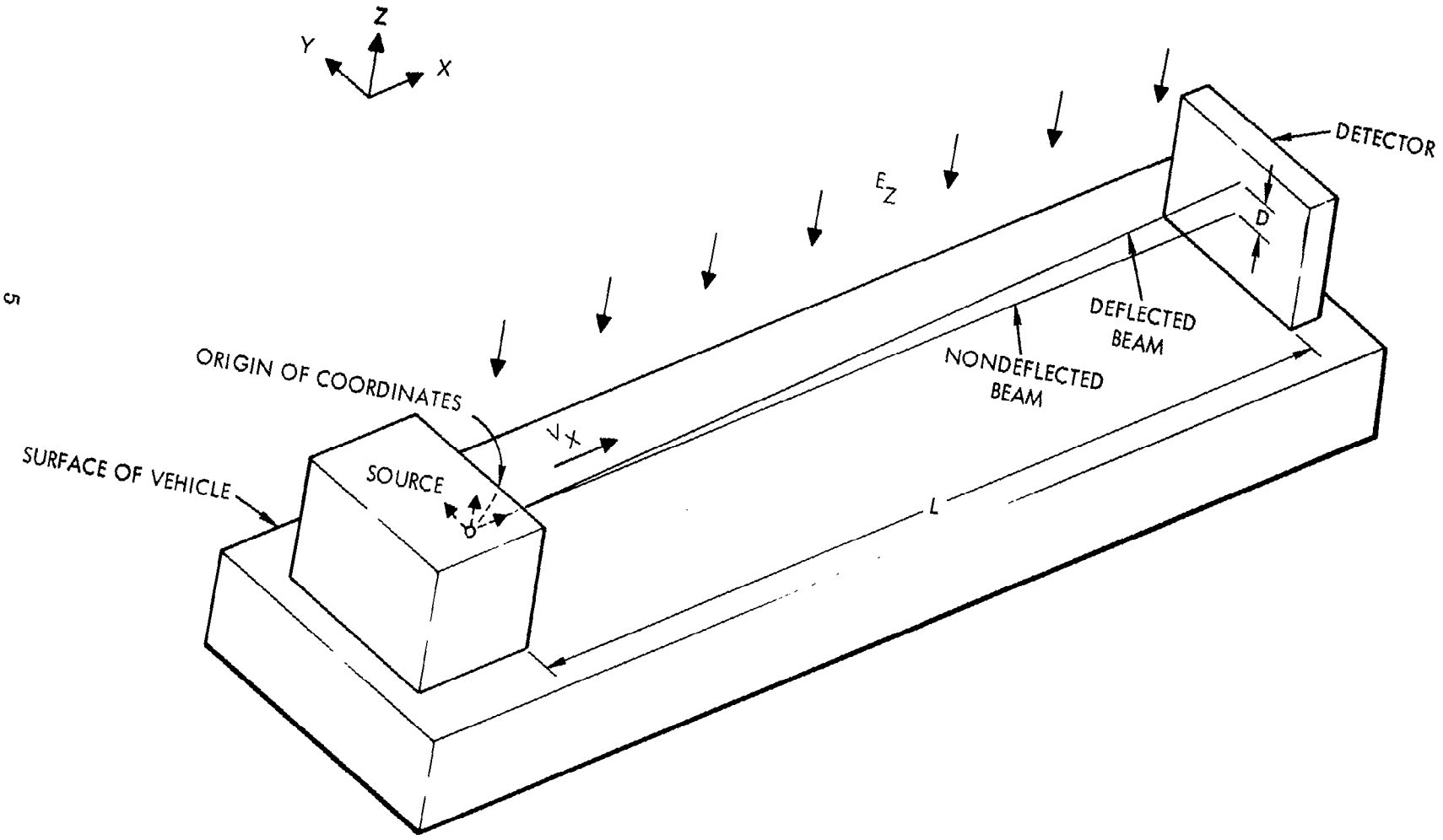

FIGURE 1 ELECTRIC FIELD MEASURING DEVICE

the deflection sensitivity increases as v_o decreases; and heavy ions because the inequality given in equation (4) is easier to satisfy for large values of m. By using heavy ions instead of electrons, the large increase in mass offers a great advantage for working in a magnetic field without loss of sensitivity in measuring the electric field. This latter statement is true since the deflection, D, of equation (5) is independent of the particle mass.

Cs ion beams are, therefore, ideal to consider since they are of high mass, low ionization potential, and the technology for handling them is well known. The ability of a Cs ion beam to measure the E_z can be seen in the following calculation. Typical values for the parameters of the system are assumed and the maximum disturbing fields that can be tolerated for any given electric field are determined.

Two systems are designed with the following parameters:

(a) (b)

L = 1.0 meter and 0.3 meters

v_o = 10 volts

$(q/m) = 7.17 \times 10^5$ coulomb/kg

For these values, it can be shown that

$$V_x = 3.81 \times 10^3 \text{ m/sec}$$

(a) (b)

$$T = L/V_x = 2.62 \times 10^{-4} \text{ sec and } 7.36 \times 10^{-5}$$

(a) (b)

$$D = (2.50 \times 10^{-2} \text{ m}^2/\text{volt})\, E_z \text{ and } (2.25 \times 10^{-3} \text{ m}^2/\text{volt})E_z$$

The deflection is given in terms of the electric field in Figure 2. Equation (6) gives the limit of the magnetic field that can be tolerated by the instrument.

$$B = (2.62 \times 10^{-4} \text{ sec/m})\, E_z \text{ X allowable error} \qquad (6)$$

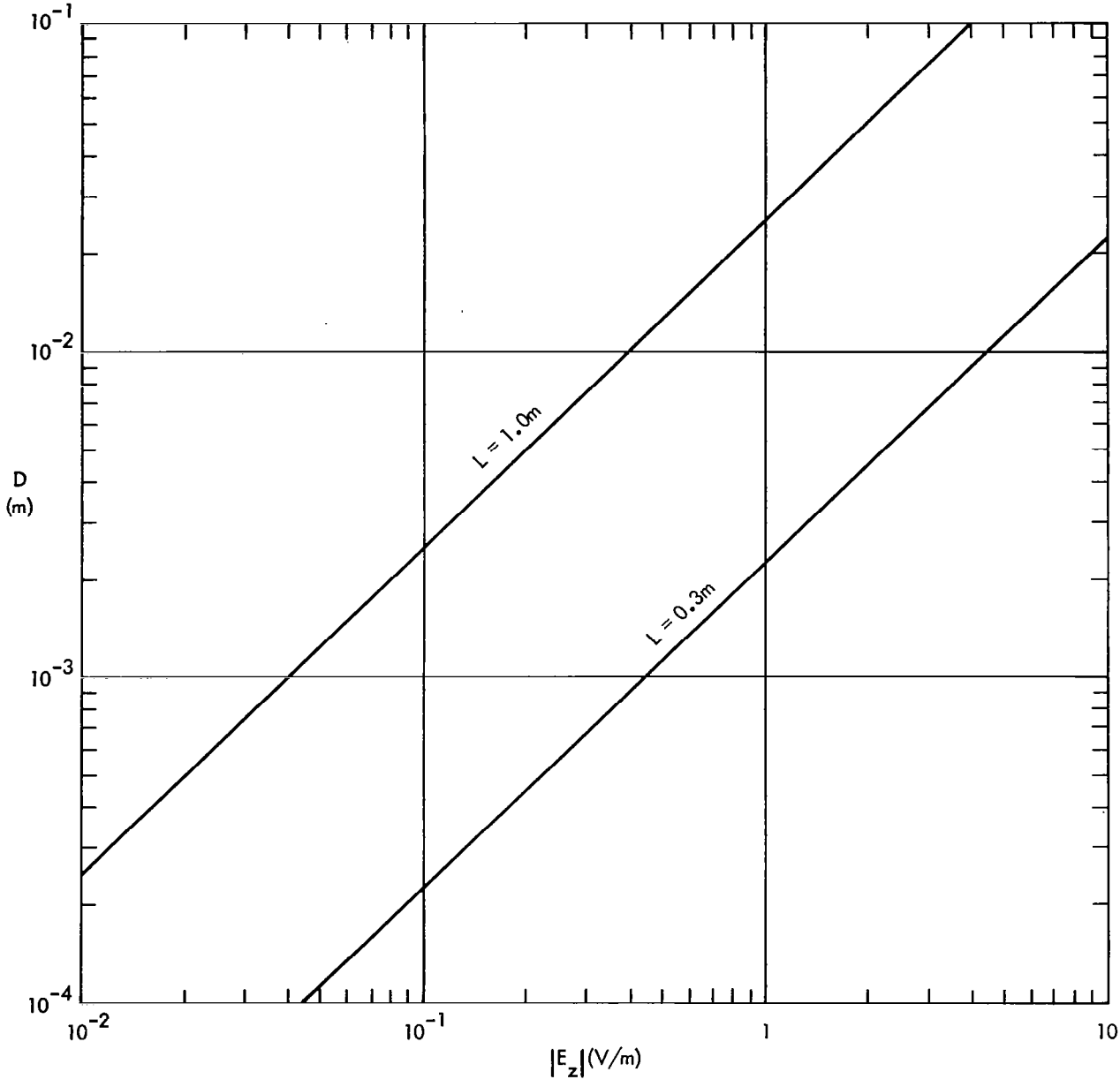

FIGURE 2 DEFLECTION VERSUS ELECTRIC FIELD

Assuming that the allowable error of the cesium ion beam measurement is ten percent, then

$$B_{max} = (2.62 \times 10^{-5} \text{ sec/m})\, E_z \qquad (7)$$

Figure 3 shows a plot of equation (7).

Calculations concerning the beam deflection show that if very small electric fields are to be measured, i.e., 10^{-2} volts/m, then it is extremely important that the source be capable of producing a very fine beam at the detector and the detector be capable of sensing very small deflections $\cong 0.001$ cm. Also, measurement sensitivity increases with decrease in particle energy; therefore, a low energy beam $\cong 10$ volts is desirable.

If electron beams are to be employed, the effect of the magnetic field on D would be increased by

$$(m_{Cs}/m_e)^{\frac{1}{2}} = \left[\frac{133 \times 1.66 \times 10^{-24}}{9.81 \times 10^{-28}}\right]^{\frac{1}{2}} \cong 500 \qquad (8)$$

Thus, a Cs ion beam can operate in magnetic fields 500 times larger than an electron beam.

2.2 CESIUM ION EMISSION*

2.2.1 Phenomonological Comments

Cesium ions are evaporated from a hot surface having a high work function and provide a convenient source of heavy ions.[10] The operational characteristics of many cesium ion sources have been investigated both theoretically and experimentally by many experimenters. However, the flow of cesium through a heated channel leading to ion emission at the downstream end is a much more complicated problem than the usual vapor flow problem. The usual flow analysis is a vapor phase analysis in which the flow is due to the gradient in vapor density through a passage of some simple shape.

*The theoretical approach employed in this section is due to Dr. A. T. Forrester.

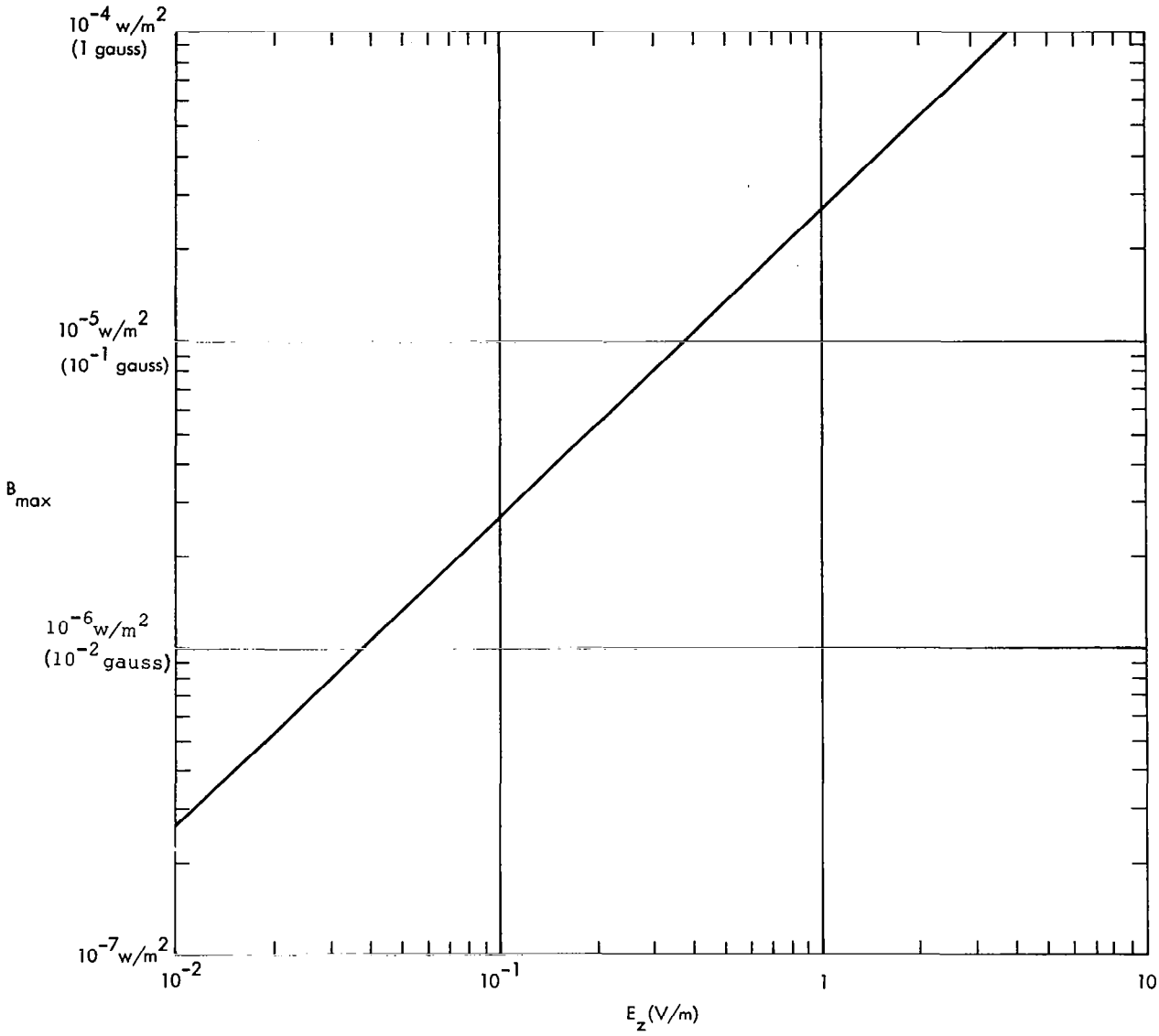

(THE DIAGONAL CURVE IS CORRECT FOR BOTH VALUES OF L.)

FIGURE 3 ALLOWABLE MAGNETIC FIELD (FOR 10% MEASUREMENT ERROR)

When flow also occurs via a second phase, a surface absorbed layer, not only does flow occur in each of these phases, but the two phases are coupled to each other through the absorption isotherms. This problem has been solved to various degrees of approximation.[10-12] One analysis[13] has taken into account the formation of a plasma inside the channel, but this only becomes significant at very high temperature ($T > 2000^{\circ}K$). At the temperatures involved in ion source applications ($T < 1500^{\circ}K$), one obtains high ion emission for low surface coverage by cesium, or high electron emission at high coverage, but there is no coverage where the emission densities of electrons and ions are sufficiently close to form a plasma of interesting density.

Of particular interest to this program is the effect of electric fields due to the varying contact potential on the heated metal surfaces of a channel through which Cs vapor passes. Although Forrester[10] has noted their effect, an analysis has not been reported in the published literature. The effect is illustrated in Figure 4. The variation of vapor density, ρ_v, and the associated density, θ, of the absorbed fractional monolayer is shown in (a). When θ is high, the work function of a cesium coated surface becomes low so that the work function varies inversely with the surface coverage (except at high coverages which are not of concern in an ion emission situation). The variation of the work function ϕ is also known in (b) in a conventional type of electron energy diagram. If temperature and electron density within the metal is assumed constant, the Fermi level is everywhere the same. In (c) the electron energy is converted to a potential which illustrates an electrostatic field in the direction of flow. If this is large enough it can have an important effect in increasing the flow of ions from a channel.

2.2.2 Space Charge Limitation

It is necessary first to consider the space charge problem since this provides the limiting conditions on ion densities. In our case, we shall consider a static problem, one in which the surface coverage θ is constant. The situation is illustrated in Figure 5.

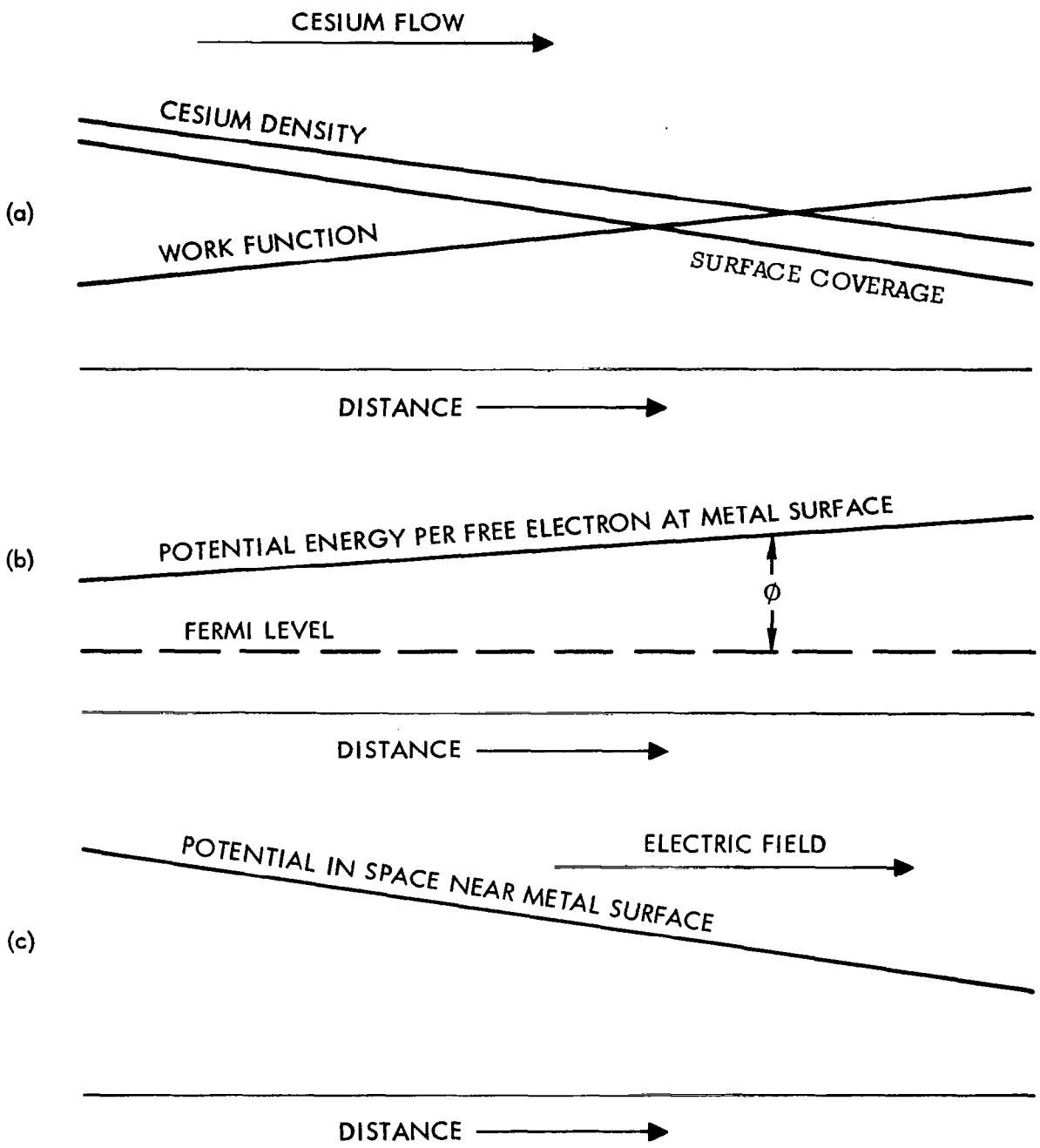

FIGURE 4 ILLUSTRATION OF THE ORIGIN OF CONTACT POTENTIAL VARIATION FIELDS IN A CESIUM FLOW SITUATION

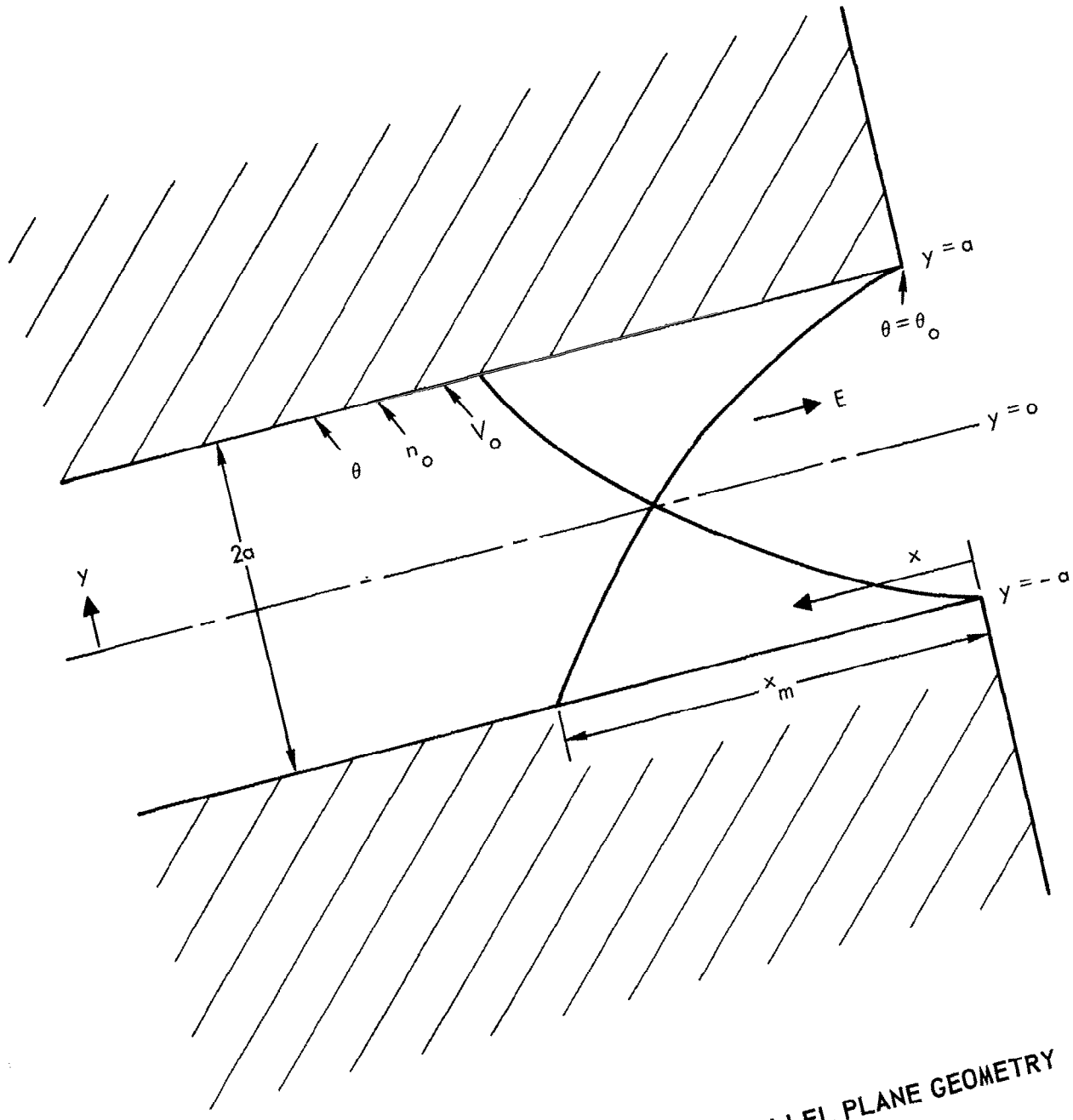

FIGURE 5 CESIUM FLOW IN PARALLEL PLANE GEOMETRY

The basic space charge equation is Poisson's equation.

$$\frac{d^2V}{dy^2} = -\frac{\rho}{\epsilon_o} \tag{9}$$

Electron densities in the vapor phase are completely negligible at temperatures of the order of 1500°K or less and Cs surface coverages of the order of .01 or less.

Equation (9) can be written

$$\frac{d^2V}{dy^2} = -\frac{qn}{\epsilon_o} \tag{10}$$

where q is the ion charge, and n is the ion density in the channel, but it is required that n vary through the channel according to the Boltzmann relation

$$n = n_o \exp \frac{(V_o - V)q}{kT} \tag{11}$$

where n_o, V_o are values of the ion density and potential at the surface. It will simplify the analysis to change to dimensionless variables

$$\eta = \frac{(V - V_o)\, q}{kT} \tag{12a}$$

and

$$\lambda = y/a \tag{12b}$$

where 2a is the channel width.

In terms of these, Poisson's equation becomes

$$\frac{d^2\eta}{d\lambda^2} = -\frac{q^2\, a^2\, n_o}{\epsilon_o\, kT} \exp(-\eta) \tag{13}$$

The condition for neglect of space charge effects on the motion of charged particles is

$$\eta \ll 1 \tag{14}$$

In this case, $\exp(-\eta) \approx 1 - \eta$ and (13) becomes

$$\frac{d^2\eta}{d\lambda^2} = -Q^2 \ (1 - \eta) \tag{15}$$

where

$$Q^2 = \frac{q^2 a^2 n_o}{\epsilon_o kT} \tag{16}$$

Equation (15) is an elementary differential equation with the general solution

$$\eta = 1 + A \exp(Q\lambda) + B \exp(-Q\lambda) \tag{17}$$

The boundary conditions for determining the constants A and B are

$$\eta = 0 \text{ at } \lambda = 1 \tag{18a}$$

$$\frac{d\eta}{d\lambda} = 0 \text{ at } \lambda = 0 \tag{18b}$$

which lead to

$$A = B = -\frac{1}{2 \cosh Q}$$

and

$$\eta = 1 - \frac{\cosh Q\lambda}{\cosh Q} \tag{19}$$

The condition (14) for low space charge is that η be everywhere $\ll 1$, which is met if $\eta_{max} \ll 1$. $\eta_{max} = \eta_\lambda = 0$ occurs at $\lambda = 0$, therefore,

$$\eta_{max} = 1 - \frac{1}{\cosh Q} \ll 1 \tag{20}$$

At $Q = 1$, $\eta = 0.35$. This is sufficiently small for the assumption $\exp(-y) = 1 - \eta$ to be valid and provides a reasonable limit to the onset of space charge as an important consideration. Thus the limit of validity of the neglect of space charge is determined by the value of $n_o = n_{max}$ satisfying

$$\frac{q^2 a^2 n_{max}}{\epsilon_o kT} = 1 \tag{21}$$

Converting n_o to the variable usually tabulated, the ion flux υ_ρ per unit area per unit time is

$$\upsilon_\rho = n_o \sqrt{kT/2\pi m} \tag{22}$$

which leads to

$$\upsilon_{max} = \frac{\epsilon_o}{\sqrt{2\pi qm}} \left(\frac{kT}{q}\right)^{3/2} \frac{1}{a^2} \tag{23}$$

where m is the mass of the charged particle, T is in ^oK, and υ_{max} is in ions per sec per unit area, so that the area units are the same as the units of a^2. T must be of the order of 1000^oK for the application here. At $T = 1000^oK$

$$\upsilon_{max} = \frac{(4.74)(10^8)}{a^2} \tag{24}$$

If contact potential variation fields are negligible the current output corresponding to this limitation is $i_\ell = 2 a q \upsilon_{max}$ per unit length of slit. Equation (24) leads to

$$i_\ell = \frac{1.52 \times 10^{-10}}{a} \text{ amperes/cm}$$

If a = 0.005 cm, then i_ℓ = 3.034 x 10^{-8} amperes/cm, which is small but adequate. It is to be hoped that the effects of electric field in the capillary will be to increase this a great deal. It is important to note that decreasing the channel width, a, increases the total current output.

Before leaving this, it should be noted that the effect computed in the next section will reduce space charge in the channel at the same time that it increases current. Therefore, the neglect of space charge may be valid out to greater values of v_ρ than given by equation (23). That assumption is, however, not being made.

Electric Field Computation

The electric field at the ionizing surface is given by

$$E = -\frac{dV}{dx} = -\frac{dV}{d\theta}\frac{d\theta}{dx}$$

For ion emission, θ is always small so that $\frac{dV}{d\theta}$ is a constant, V_o', evaluated at $\theta = 0$. For tungsten, V_o' is $-$ 10.679 and is independent of temperature.

The value of $d\theta/dx$ at the ion emitting end of the channel can be related to θ_o at that point by matching to the front face solution. This process is illustrated in Figure 5. On a plane surface where the fraction of evaporating particles returning is negligible, the solution for θ is an exponential decay with a diffusion length, δ. The derivative at each point is θ/δ.

The value of θ and its derivative must both match the front face values, so that $d\theta/dx = \theta_o/\delta$ just inside the channel. The derivative (θ_o/δ) is not necessarily constant inside the channel, but as a convenient first order computation, we will assume this to be the case, at least over the depth of the channel from which appreciable ions emerge.

Effective Depth of Emitting Surface

At ion densities corresponding to $\rho_v = 10^{-19}$ particles/cm^3. the mean free paths are very long compared to the channel thicknesses, and

the average time t for a particle to cross the channel is easily calculated. In this time the particle is caused to move downstream by the electric field a distance of $\left(\frac{qE}{m}\right) t^2$, as illustrated in Figure 5. Consider that all ions emitted over the length $x \leq X_M$ are emitted ions.

Since all variations in transit time and all initial velocities are neglected this is only an approximate treatment. The exact solution can be written down without very much difficulty, but this solution should provide valuable information on a first order approximation, provided it predicts a current large compared to the random current from the end corresponding to θ_o, i.e., as long as

$$\int_o^{x_m} \upsilon\rho\left(\theta_o + \frac{\theta_o}{\delta} X\right) dx > a\, \upsilon\rho\,(\theta_o) \tag{25}$$

Transit Time Calculation

The average value of $(1/v_y)$ for particles emerging from the surface is given by

$$\left(\frac{1}{v_y}\right)_{av} = \frac{\int_o^\infty \frac{1}{v_y} v_y \exp\,(-\tfrac{1}{2} m v_y^2/kT) d\, v_y}{\int_o^\infty v_y \exp\,(-\tfrac{1}{2} m v_y^2/kT) d\, v_y}$$

This leads through tabulated integrals to an average transit time of

$$t = 2a \left(\frac{1}{v_{av}}\right) = a\sqrt{\frac{2\pi m}{kT}} \tag{26}$$

Current Calculations

Since the electric field is given by $V_o'\theta_o\delta$

$$x_m = \frac{\pi e V_o' a^2}{\delta kT} \theta_o \tag{27}$$

The emission from the channel is therefore given by

$$i_\ell = 2q \int_o^{x_m} \nu\rho \left(\theta_o + \frac{\theta_o}{\delta} x\right) \quad dx \tag{28}$$

or

$$i_\ell = 2q \frac{\delta}{\theta_o} \int_{\theta_o}^{\theta_o + \frac{\theta_o}{\delta} x_m} \nu\rho\,(\theta) d\theta \tag{29}$$

Equation (29) permits studying the current output of the source design considered in the present program. A more exact solution has been effected, but further studies involving an evaluation of equation (29) and more exact solutions will have to be performed in the future.

SECTION 3.0

DESCRIPTION OF THE EXPERIMENT AND DATA ANALYSIS

A cesium ion beam electric field measuring instrument consists of the cesium ion source, detector, and electronic readout system. In addition, the experiment performed to test this device utilizes a pair of deflection plates for ion beam calibration and diagnostics. The experiments are performed in an 18 inch diameter by 30 inches high metal screen-covered bell jar, using a Veeco VS 400 vacuum system. Figure 6 shows the physical layout of the experiment.

Cesium atoms evaporated from a hot tungsten surface or other similar metals with high work functions leave the surface as ions.[10] The evaporation of cesium from hot porous tungsten surfaces is presently being successfully used in contact ion thrusters as an efficient and reliable ion source. The design constraints, however, for a cesium ion source used to measure electrostatic or low frequency electric fields are considerably different from those of an ion thruster principally because in the former, low currents $\sim 10^{-9}$ amps and a well focused beam with a very low accelerating voltage, $\sim$ 10 volts, are required. In addition, these sources should be capable of operating at a power of a few watts.

The first cesium ion source employed in these studies under Phase I of this program is a radiant heated source, i.e., the ionizer is heated by the radiation from a hot filament. Figure 7 is a schematic of this source showing the ionizing region only. The ionizer is formed into a thin slit approximately 0.004 inches wide, formed by flattening a 3/16 inch diameter, 0.015 inch wall tantalum tube around a thin shim. The cesium ion beam exiting the ionizer is thus in the shape of a ribbon which permits small deflection measurements with currents higher than

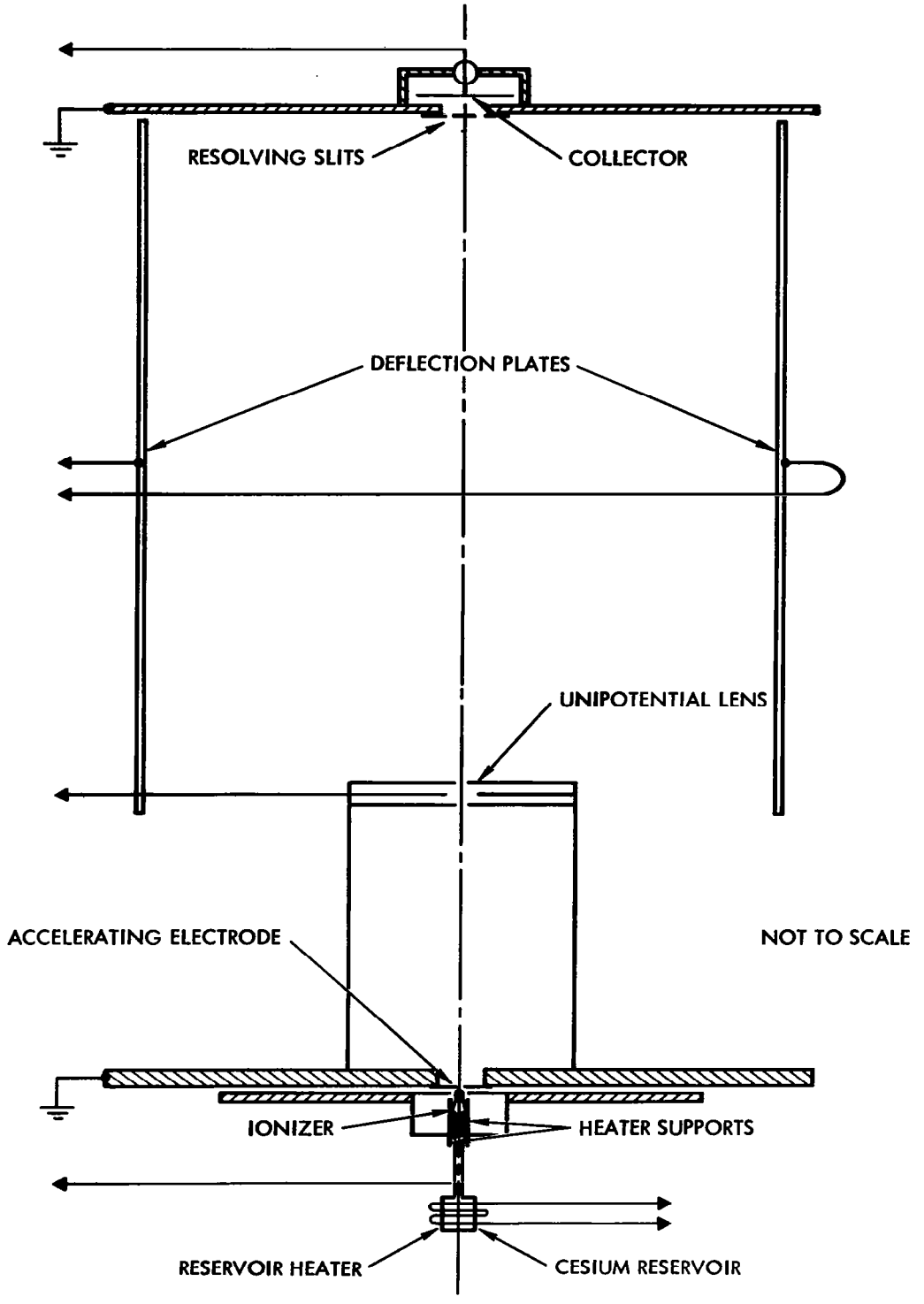

FIGURE 6 SCHEMATIC OF ELECTRIC FIELD EXPERIMENT

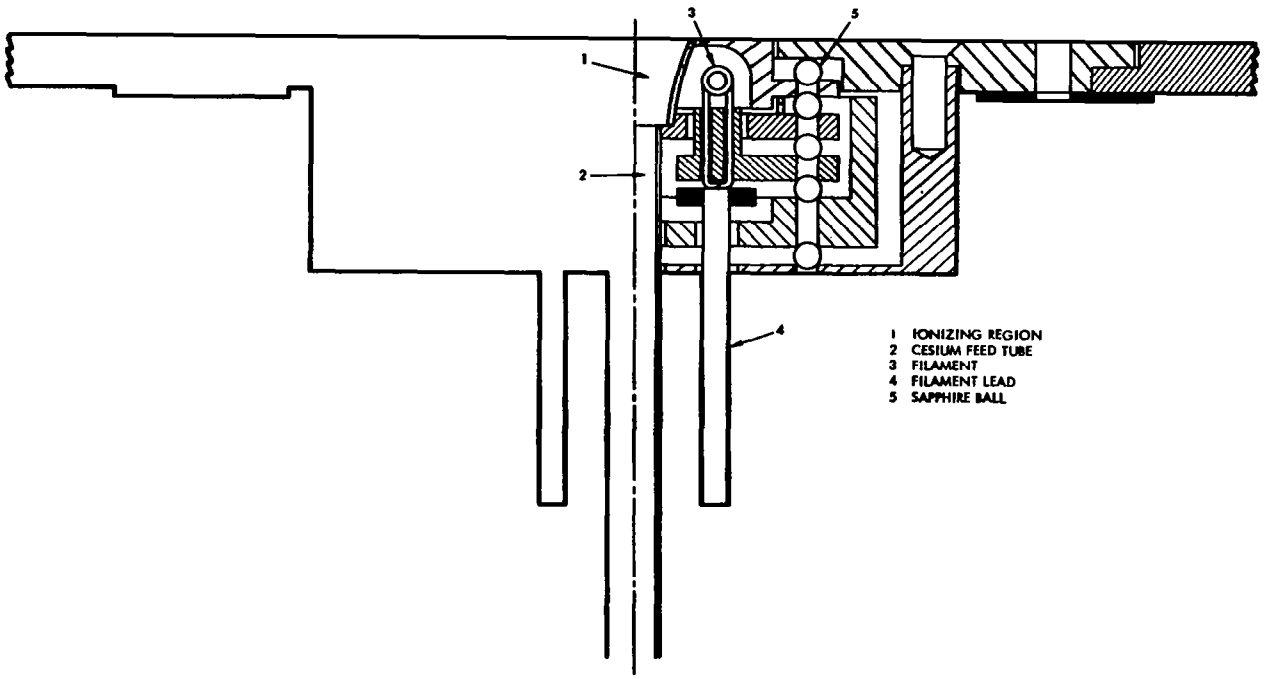

FIGURE 7 RADIANT HEATED SOURCE

would be obtained with a pencil shaped beam. Tantalum is used here because of its ductility, machinability, high melting point, and high work function. Cesium is fed to the ionizer through a 1/8 inch tantalum tube. Both this tube and the ionizer are electron beam welded to a common connector, tantalum being used here for all three parts to eliminate any welding problems.

The heater is a 0.015 inch diameter tungsten - 3% rhenium wire in the form of two semicircular coils connected in parallel surrounding the ionizer. Nickel parts are used to support and provide current to the heaters. In general, commercially pure nickel is used for intermediate temperature service because its high thermal conductivity and low coefficient of thermal expansion minimize thermal distortion. The low temperature components are made of stainless steel. Precision sapphire balls are used to provide thermal and electrical insulation and to insure that the original alignment can be reproduced on reassembling the unit. Figure 8 is a top view of the assembled source.

As part of Phase II, a second cesium ion source was constructed, based somewhat on the experience gained from testing the radiant heated source, but designed principally to test another method for heating the ionizer. The radiant heated source requires a relatively large filament which, because of heat shield limitation, raises some external components to relatively large temperatures resulting in considerable heat loss. The new design replaces the coiled filament with two straight 0.005 inch tungsten - 3% rhenium wires suspended between two nickel posts with one wire on each side of the ionizer. Electrons emitted from the filament are used to heat the ionizer by bombardment to provide localized heating on the desired component. Also, an additional radiation shield is inserted around the filament to reduce heat leakage and which is also electrically connected to repel electrons toward the filament and ionizer. This component is referred to as the counter electrode. Thus, in this design, only two components are heated to a high temperature; the filament and ionizer. Figure 9 is a cross sectional scale drawing of the electron bombardment heated source (EB source). Figures 10, 11, and 12 show photographs of the EB source components in various stages of assembly.

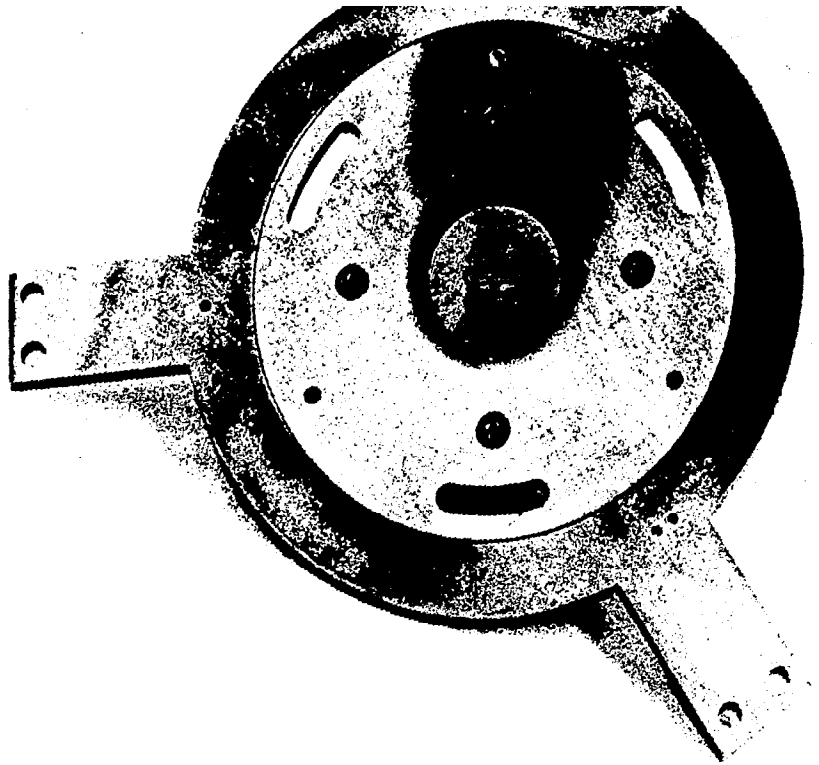

FIGURE 8 ASSEMBLED SOURCE (TOP VIEW)

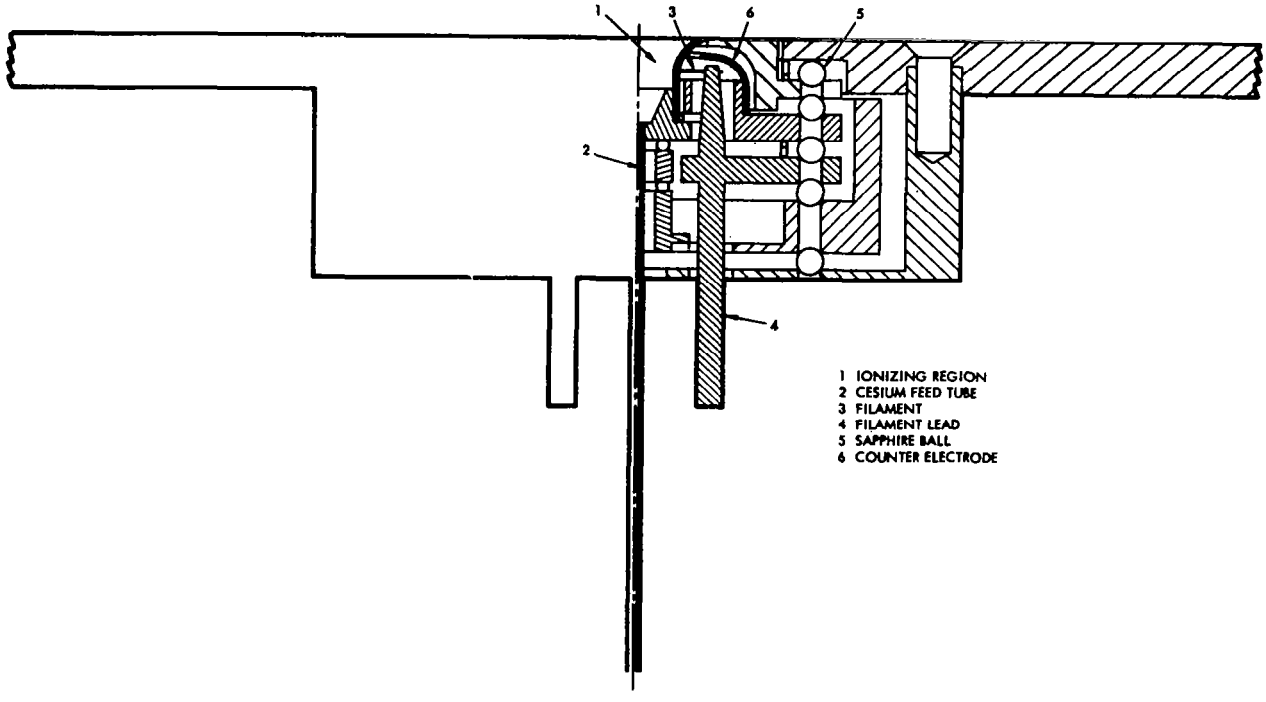

FIGURE 9 ELECTRON BOMBARDMENT HEATED SOURCE

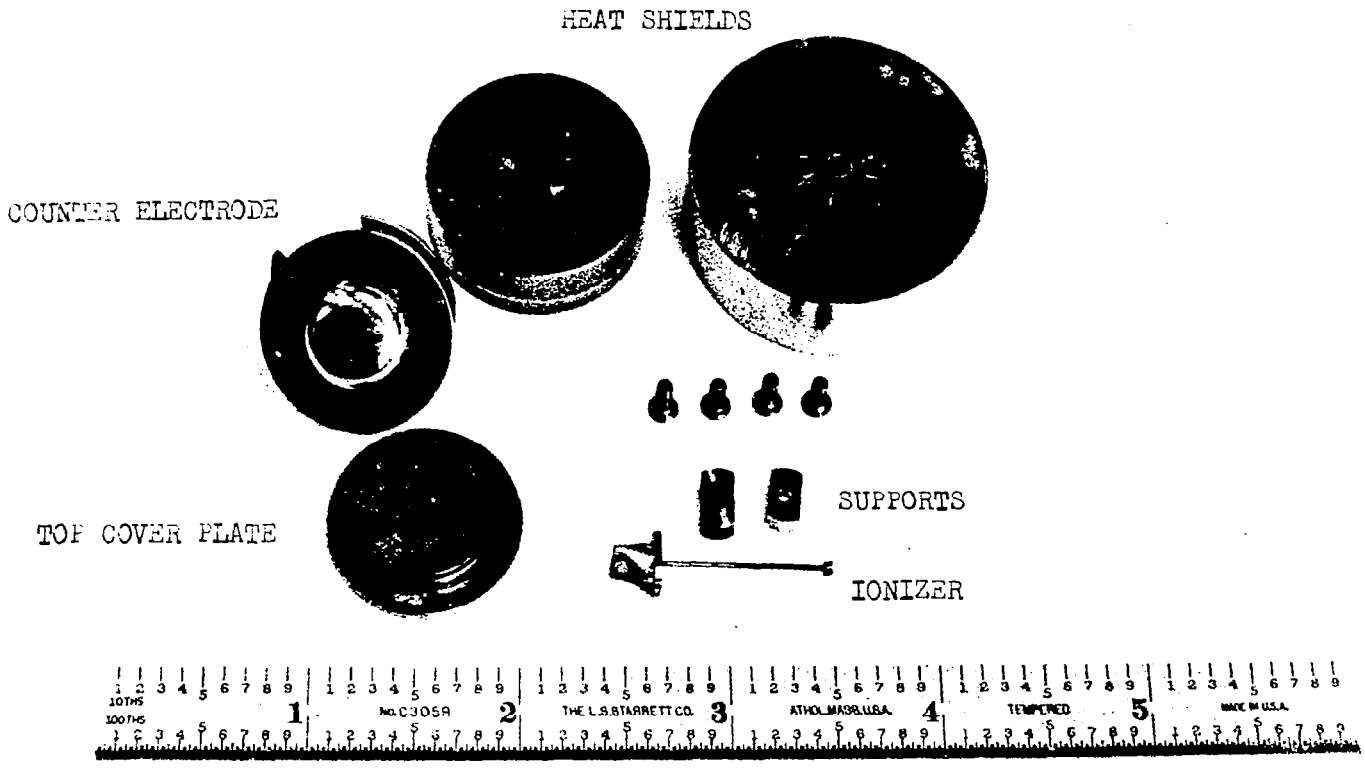

FIGURE 10 SOURCE COMPONENTS

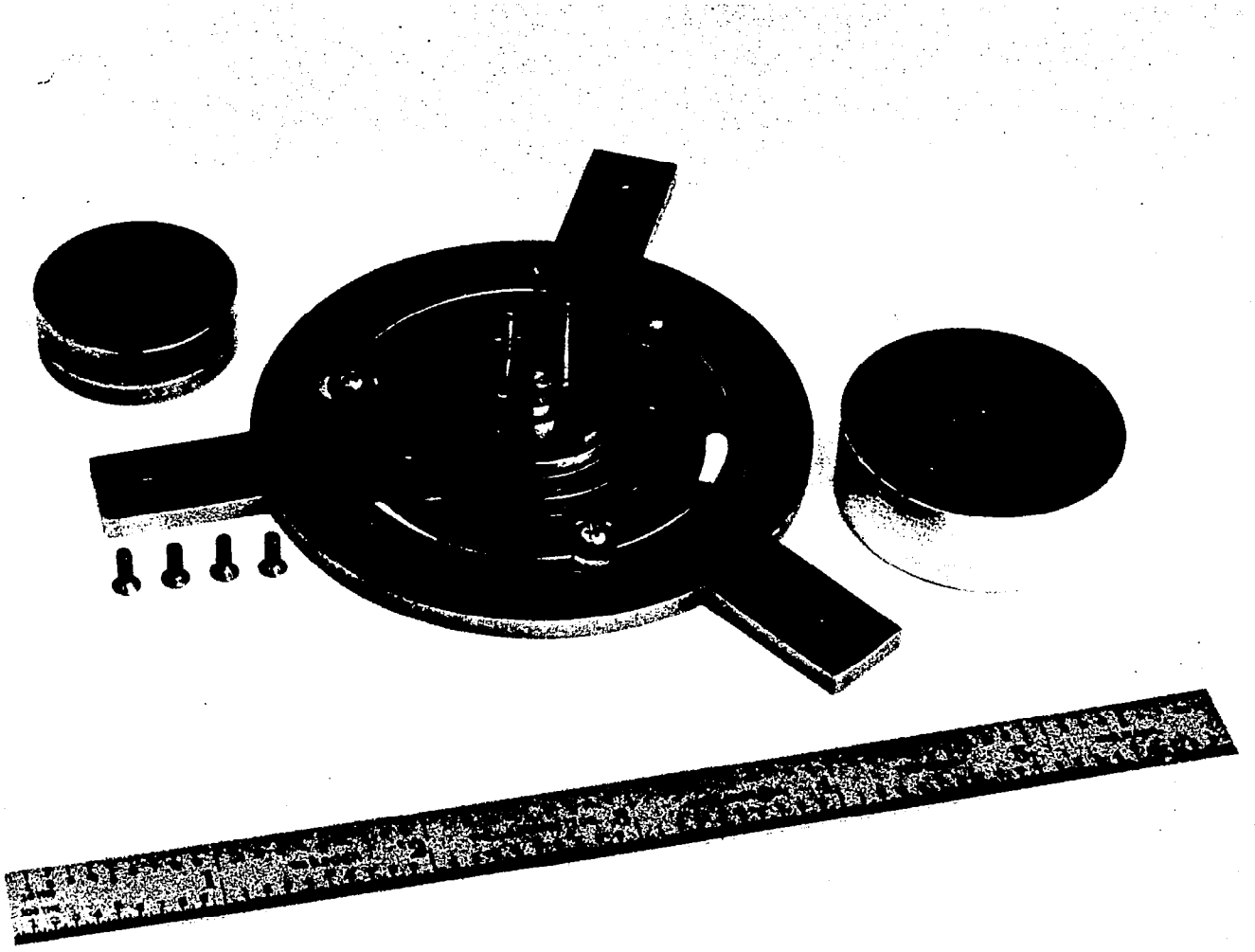

FIGURE 11 PARTIALLY ASSEMBLED SOURCE

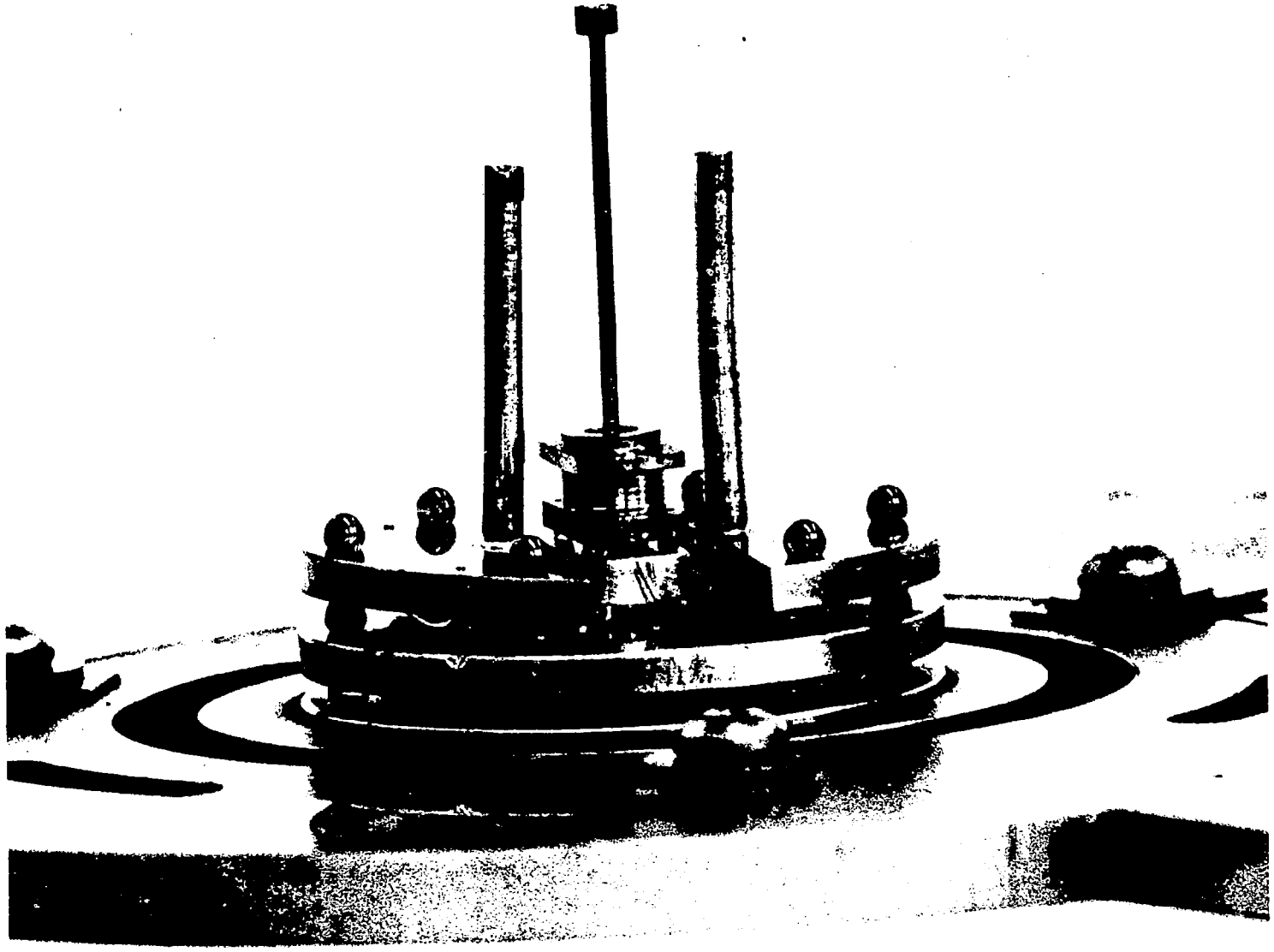

FIGURE 12 PARTIALLY ASSEMBLED SOURCE (BOTTOM VIEW)

Both sources have provision for electrically heating the cesium reservoirs positioned at the bottom of the cesium feed tube. The reservoir for the EB source also had provision for water cooling since, in the experiment previously performed with the RH source, the heat conduction to the reservoir was too large, causing excessive flow of cesium to the ionizer. Additionally, the tantalum feed tube diameter for the new EB source is reduced to 0.015 inches inside diameter to help reduce the cesium flow rate to the ionizer. The accelerating electrode is a molybdenum slit 0.015 inches wide aligned 0.040 inches above the ionizer. A unipotential lens is supported at the top of a stainless steel cylinder for focusing the beam at the detector. The detector consists of a resolving dual slit plate positioned in front of an insulated collector plate. The two parallel resolving slits are each 0.030 inches wide set 0.100 inches center to center apart. Two large stainless steel plates are positioned 2.2 inches on either side of the ion beam to serve as deflecting electrodes. The deflecting voltage is balanced with respect to ground and is adjustable from −25% through zero to +25% of the supply voltage. The supply voltage itself can be varied from 0 to approximately 40 volts. This arrangement provides great flexibility in taking the experimental data in that very precise small changes in the electric field can be made over a large range of values. Figure 13 is a photograph showing the test assembly outside of the bell jar.

The current to the collector plate is fed through a Keithly amplifier and the output is displayed on an X-Y recorder. By automatically varying the voltage across the deflection plates, the beam is correspondingly deflected across the two slits producing collector current peaks as a function of deflection voltage. Deflecting a single narrow beam across the dual resolving slit results in two separate current peaks. Figure 14 is an example of the data taken with the RH cesium ion source. It can be observed that the ion beam produced by the source is a single peak superimposed on a broader but less intense beam having a complex structure. Actually, the data in Figure 14 has the best resolution of all the data observed with the RH source, and was taken with a source input power of 31 watts. Data

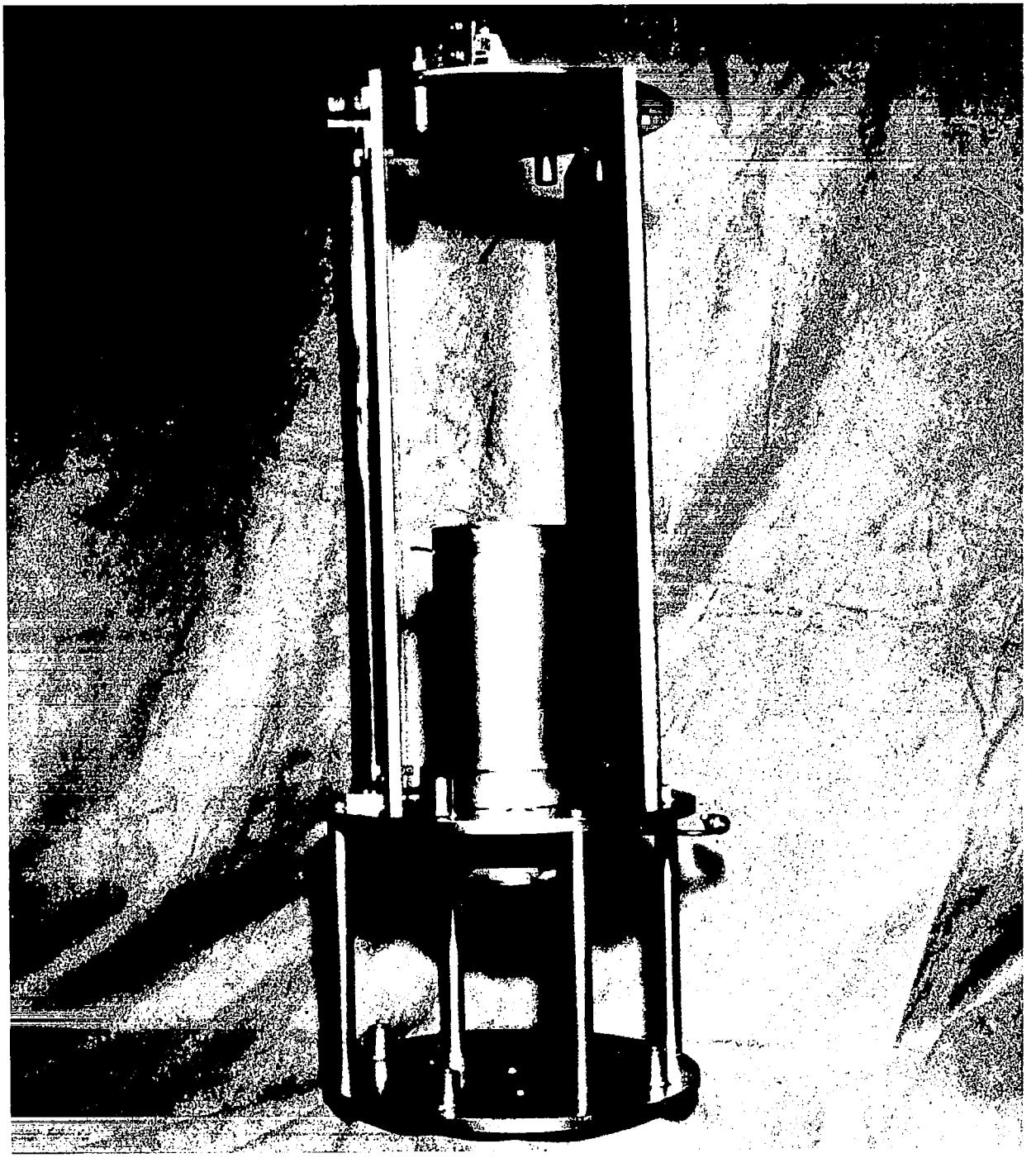

FIGURE 13 TEST ASSEMBLY

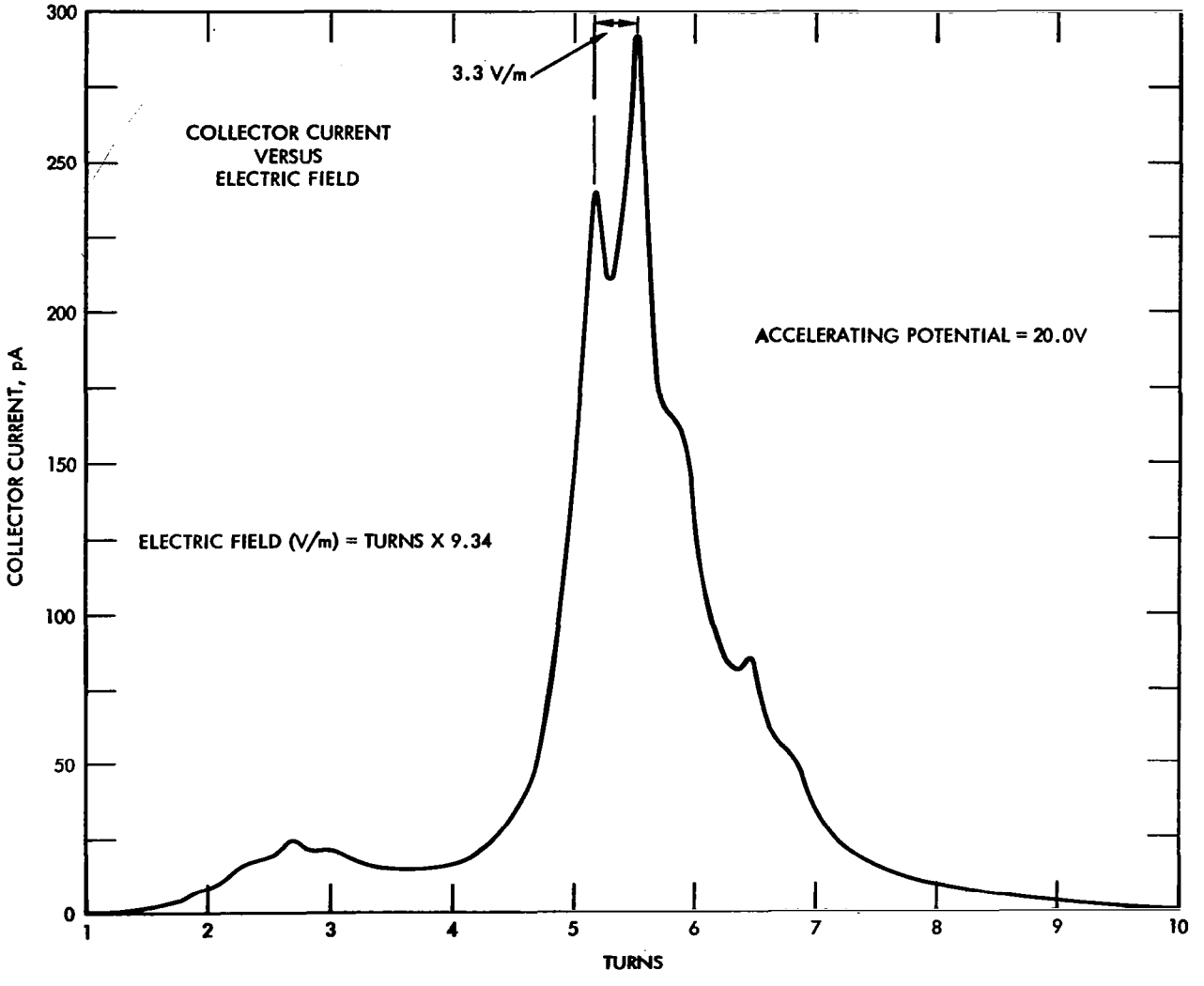

FIGURE 14 RADIANT HEATED SOURCE DATA

taken at a lower input power showed three distinct current peaks each of which were separated into two peaks by the detector slits. As the power input and ionizer temperature were increased, the intensity of the two side peaks decreased relatively to the center one. The two outer cesium ion beams are probably due to an excessive cesium flow rate to the ionizer covering the tantalum tube slit edges with cesium which, when evaporated, generated the two side beams. On heating the ionizer, the cesium coverage of these edges were reduced lowering the cesium ion currents originating from these regions while, at the same time, the inner walls of the slit become more effective in producing cesium ions and this increases the intensity of the center beam. Since this source did not have provision for cooling the reservoir with water, the minimum cesium flow rate was determined by the heat transport along the cesium feed tube and this was excessive. The RH source can produce a copius supply of cesium ions as was verified by increasing the accelerating voltage to 600 volts and observing a total current output of 2×10^{-6} amperes. The accelerating voltage-collector current relation obtained in this manner obeyed Child's law approximately, establishing that the RH source was space-charge limited.

The two principal peaks in Figure 14 represents the passage of the main peak past the dual collector slit. The abscissa of Figure 14 is scaled in terms of turns of a ten turn potentiometer and each turn represents a change in the electric field of 8.84 V/m. Consequently, the peak separation of 0.35 turns represents a change in electric field of 3.1 V/m. Solving the deflection equation (equation (30)) for L, the effective length of the deflecting field can be computed

$$L = \sqrt{\frac{4\, v_o\, D}{E}} \qquad (30)$$

In this equation, v_o is the accelerating potential, D is the beam deflection and E is the electric field intensity. For the data in Figure 14, v_o = 20 volts, $D = 2.54 \times 10^{-3}$ meter (0.1 inch), and E = 3.10 V/m so that L = 10 inches. This is somewhat larger than expected since the

distance between the equipotential lens and the resolving slit is only 9.5 inches. However, there are several reasons for this discrepancy which are discussed in the last section of this report.

It is interesting to compute the expected electric field directly from the measured deflection, assuming the electric field is effective for 23 cm, the length of the deflection plates. In this case, an electric field of 3.84 V/m is anticipated.

A large improvement in beam structure is obtained with the EB source in that the beam is sufficiently well focused to produce two distinct peaks as the beam passes the resolving slits as shown in Figure 15. A special mechanical shutter was installed to permit a remote interception of the beam in front of one slit. Data taken with one slit covered with this shutter is presented in Figure 16, verifying that the two peaks are indeed a single ion beam being deflected across the two slit.

A similar analysis to that performed for the Figure 14 data can be made for these data. Here the peak separation is 9.99 V/m when the accelerating voltage is 21 volts. This gives an L = 5.76 inches and an E = 4 V/m. There is a large discrepancy here and it is opposite to that obtained for the previous case. In this case, the electric field across the deflection plate appears to be high by a factor of $2\frac{1}{2}$ or the electric field between the plates has an effective length of 63% of that of the deflection plates. Data were taken at other accelerating voltages using the EB source and the same large relative error persisted; consequently, the data indicated some error associated with the deflecting plate voltages. A post data inspection of the equipment was made and it was discovered that a lead to one of the deflection plates had been severed. Thus, an error factor of a little more than two in the magnitude of the electric field is understandable.

When the accelerating voltage is changed, the beam becomes defocused and it takes a few hours for the system to be brought back into equilibrium and focus. Consequently, considerable time was used in taking the first set of data with the various sources. After taking the first set of data with the EB source, the filament opened terminating the

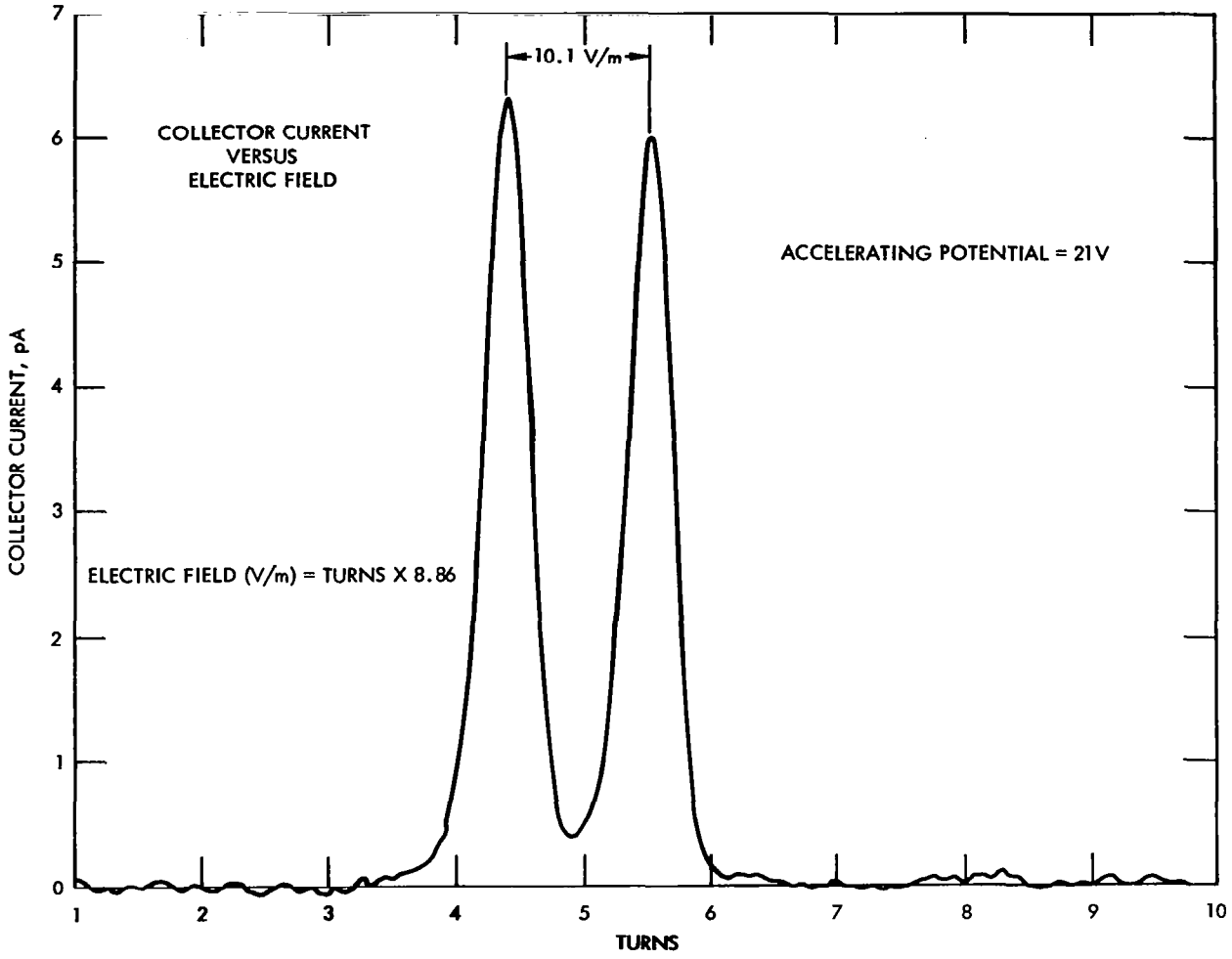

FIGURE 15 ELECTRON BOMBARDMENT HEATED SOURCE DATA

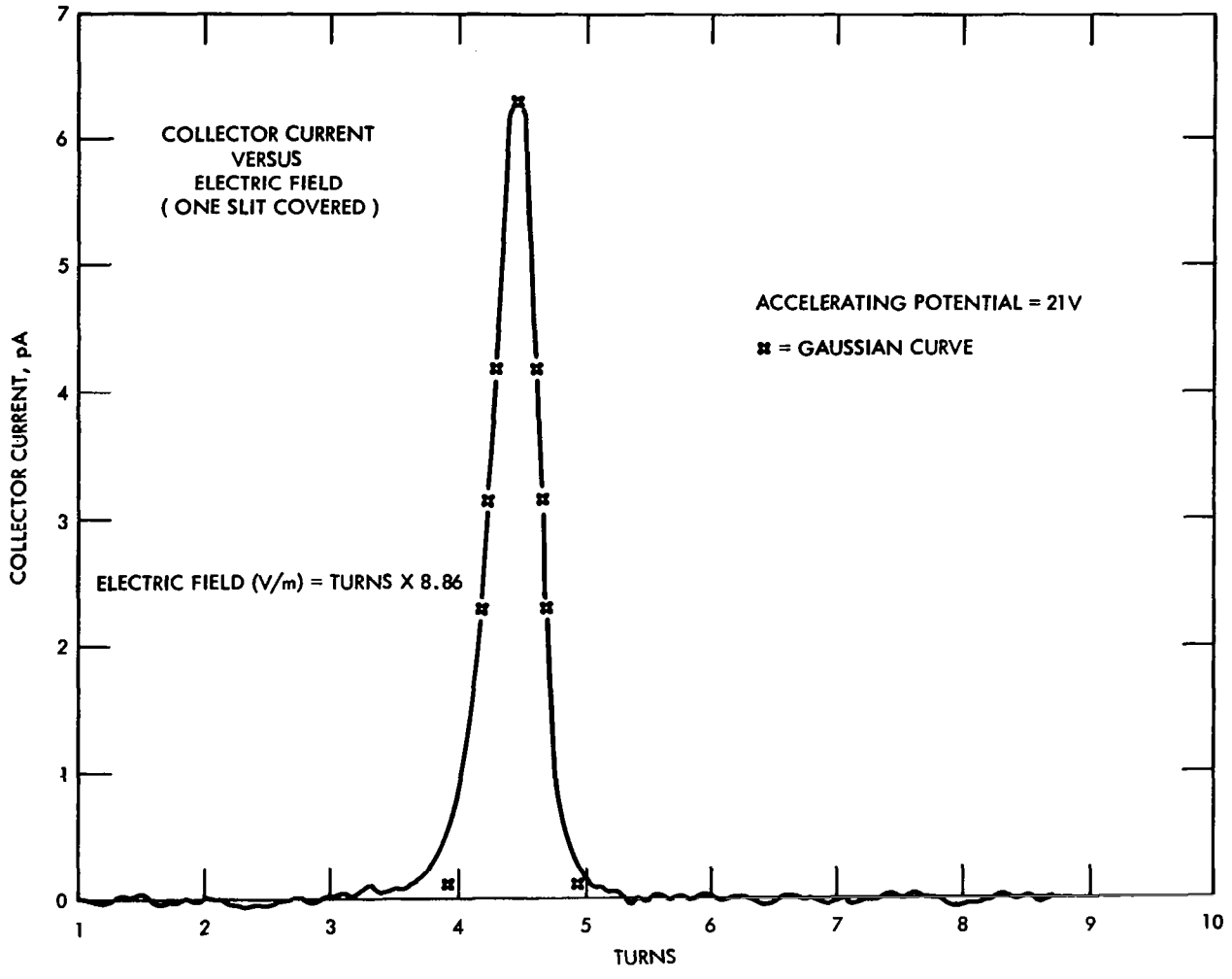

FIGURE 16 EB SOURCE DATA (ONE SLIT COVERED)

experiments. The discovery of the broken wire to the deflection plate, as stated, was made after the experiment had been terminated and, consequently, a rerun of the experiment could not be made within the alloted schedule.

Previous data taken with the RH source showed that the calculated deflection of the beam agreed with the measured value within 10%, i.e., data taken with the RH source. This being the case, one turn equals 3.54 V change in the electric field. Since the center of the peak can be defined to 0.01 turns, this instrument can attain a precision of 0.035 volts/meter. This is by no means the maximum capability of this instrument, since there are many ways to improve the precision of this device as discussed in the last section of the report.

The power consumption of the radiant heated source varies between 25 watts and 50 watts, the better data being taken at the 50 watts power input. The EB source operated between 12 watts and 22 watts with the filament utilizing 7 watts alone. It is anticipated that the 7 watts to the filament can be greatly reduced by using different heater materials and a ribbon shaped filament to provide more electrons at a lower filament temperature. Replacing the nickel filament supports with thinner molybdenum studs should reduce the heat leakage from the filament. By this and other methods it is believed that the EB source used in these experiments can be modified to give accurate electric field data when operating near 12 watts.

The shape of the curve shown in Figure 16 is gaussian except at the very low currents providing a simple means for determining the actual beam shape.

Let

$$Y = Y_o \exp - \frac{X^2}{2\sigma^2} \tag{31}$$

represent the actual beam shape. Then the current, $I(D)$, as measured for any beam deflection, D, is

$$I(D) = \int_{-x_o}^{+x_o} Y_o \exp\left(\frac{(X - D)}{2\sigma^2}\right) dx \qquad (32)$$

where x_o is half the slit width (0.015"). The data of Figure 9 represents I(D) where

$$I(D) = I_o \exp - \left(\frac{D^2}{2\sigma_s^2}\right) \qquad (33)$$

and σ_s = 0.187 turns. An analysis of the data shows that for the actual beam

$$\sigma = 0.145 \text{ turns.}$$

The parameter σ is related to the beam width at half-maximum, x_1, by

$$0.5 = \exp -\left(\frac{x_1^2}{2\sigma^2}\right) \text{ or } \sigma = 0.849\ x_1$$

It follows that for the beam prior to entering the resolving slit

$$x_1 = 0.171 \text{ turns} = 0.015 \text{ inches.}$$

Thus the beam width at half-maximum is equal to the width of one of the resolving slits.

SECTION 4.0

DISCUSSION OF RESULTS AND CONCLUSION

There are difficulties in obtaining the electric field in space because of the perturbing effects produced by the vehicle itself. However, the more sensitively and accurately one can measure fields at the surface of a vehicle, the more accurately one can infer the unperturbed electric field. The cesium ion beam electric field meter appears to provide a very promising approach to this problem.

In addition to the prospect of increased sensitivity and accuracy, with respect to such instruments as field mills, it offers the interesting possibility that perturbations may be avoided in some cases. This might be achieved by sending the ion beam through a portion of space relatively far removed from the vehicle by having the ion source and ion detectors on two separate extensions.

These speculations are somewhat beyond the scope of this program which covered the demonstration of the practicality of using an ion beam as a sensitive field sensor. This has clearly been established.

In the flight instrument, an electronic data readout system is required to provide a data link with the satellite or rocket. The one presently proposed is that shown schematically in Figure 17. A set of deflecting electrodes is incorporated as an integral part of the cesium ion beam source to center the beam on a single slit. The ambient electric field is determined by measuring the voltage applied to the deflecting electrodes to maintain the ion beam centered on the detector slit. The circuit is a two-mode, self-adaptive, closed loop control system. The two modes consist of a proportional mode for beam finding

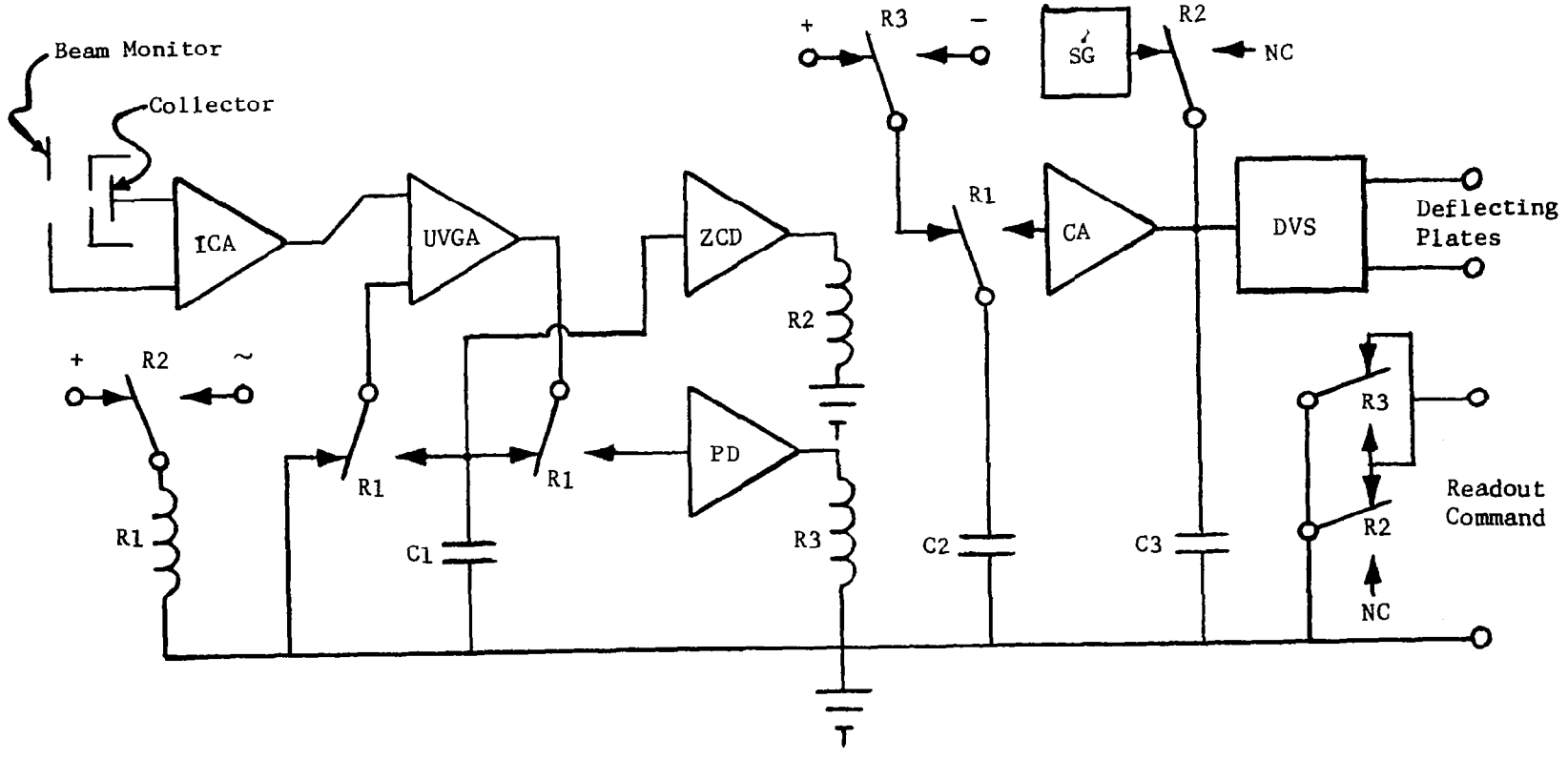

FIGURE 17. ELECTRONIC MEASURING SYSTEM

and a rate mode for locating the center of the beam. The system operates in the proportional mode only during system start up, or in case some system transient results in loss of the beam. Otherwise, as explained below, the rate mode operates so as to track the beam. In the proportional mode, a periodic sweep generator (SG) drives the deflecting voltage supply (DVS) from one extreme to the other. The system switches to the rate mode when the collector current exceeds some large fraction of the maximum beam current. In the rate mode, the collector current is sampled for one-half of a sampling period, the deflecting voltage is incremented by a small amount, and the collector current for the second half of the sampling period is then compared with the sampled value for the first half period. The result of this comparison changes sign when the increment shifts the ion beam past the center of the resolving slit. The value of the deflecting voltage at this instant in time is the value representative of the unknown electric field. Each time the comparison changes sign, the polarity of the increment applied to the deflecting voltage supply is also changed so as to continuously track the unknown electric field.

The best data taken with the RH source (Figure 14) did produce two resolved current peaks that were superimposed on a broader but less intense current background. This background current is due principally to an excessive cesium flow rate to the ionizer. As a consequence, the exit port of the ionizer was flooded with cesium, allowing the two edges of the ionizer tube to become a source of cesium ions. By heating the ionizer to a higher temperature, the extraneous sources were minimized resulting in the data picture of Figure 14.

The effect was eliminated with the EB source where the cesium flow rate was reduced by water cooling the cesium reservoir and by greatly reducing the diameter of the cesium feed tube connecting the reservoir to the ionizer. The inside diameter of the cesium feed tube is only 0.015 inches, and if pure cesium is used in the reservoir, some reduction in tube diameter may be required. A better approach may be to use some additive to the reservoir which essentially decreases evaporation of

cesium at a given temperature. Cesium absorbed on charcoal, "cesium-tin mixture", or some cesium compound that dissociates at 100°C or above may be satisfactory.[14] Operation of the cesium reservoir at a higher temperature is mandatory for a flight instrument since the reservoir will operate at a temperature equal to or greater than that of the spacecraft temperature. Designing smaller ID feed tubes into the system can be achieved, however, without great difficulty.

The deflection of the beam measured with the RH source is approximately 10 to 15% greater than expected. Although a complete experimental analysis for the data has not been made, a total error of this magnitude can be expected. The voltage readings themselves have a probable error of $\pm$ 5%, and the contact potential and space charge effects at the ionizer exit can introduce uncertainties in the value of the ion energy to account for the remaining error.

The data taken with the EB source exhibits an almost perfect gaussian shape. The noise current is almost all generated in the collector current (probably by piezoelectric effects in the dielectric of the cable connecting the collector plate to the amplifier). By increasing the collector current thereby increasing the signal to noise ratio, the ultimate sensitivity of this instrument can be improved since its sensitivity is determined by the peak signal-to-noise ratio. The electronic circuit for the flight instrument maintains the beam centered on the detector slit by finding the point of zero slope. Even at the peak signal to noise ratio obtained with the present EB source and associated electronic circuitry, the beam center can be determined to within 0.01 turn or approximately 0.002 cm. This results in a measurement of the electric field to a precision of 0.035 V/m. Further improvement in the precision of the present device can be made by:

1) decreasing the width of the ionizer slit,
2) increasing the cesium ion current to noise ratio,
3) increasing the length, L, the distance the beam travels exposed to the field,

4) using different focusing techniques,

5) changing the accelerating voltage.

Theoretical studies show that for a current limited source, decreasing the width dimension of the slit, all other conditions remaining the same, will actually increase the current. The change in the work function of a fractional monolayer cesium covered surface leads to the formation of an electric field in the slit channel which becomes part of the accelerating voltage. This effect, together with the beam broadening effects of thermal energy spread, space charge, gas pressure, and residual angular aberration determine the degree to which the beam can be sharply focused on the detector slit. The ability of the lens to focus the beam into a small slit increases with increasing accelerating voltage since the thermal effects will be minimized; however, the beam deflection sensitivity is reduced. Nevertheless, some improvement in sensitivity may be gained here, particularly if longer beam paths and different focusing methods are investigated.

The EB source offers the greatest advantage for use with a flight instrument because of its lower power consumption and faster start up time. An actual flight source should be smaller than the lab models presented in this report and will operate on considerably less power. Nevertheless, filaments with greater electron mission efficiency at lower temperatures should be investigated. It is anticipated that an acceptable instrument could be effected that operates on 5 watts or less.

In conclusion, sufficient information has been gained during this program to design a lab model of a flight instrument that will measure electric fields of the order of 0.01 volts/meter in space. However, it will be necessary to study, (1) methods for reducing the power requirements through improved filament design, (2) techniques for reducing cesium flow rate with higher reservoir temperatures, (3) operational methods for optimizing and building the electronic readout system, and (4) environmental tests with prototype instrument before a flightworthy cesium ion beam electric field meter can be constructed.

REFERENCES

1. Chalmers, J. Alan, "Atmospheric Electricity," Permagon Press (1957).

2. Chalmer, J. A., Hutchinson, W.C.A., Wildman, P.J.L., and Edwards, M. G., "Measurement of Low Electric Fields Under Upper Atmosphere Conditions," University of Durham, Report for U.S.A.F. Cambridge Research Center, AD 418211, (November 1962).

3. Vonnegut, B., Moore, C. B., and Mallahan, F. J., "Adjustable Potential-Gradient-Measuring Apparatus for Airplane Use," J. Geophys. Res., 66, No. 8, 2393-2397, (August 1961).

4. Paltridge, G. W., "Measurement of the Electrostatic Field in the Stratosphere," J. Geophys. Res., 69, 1947-1954 (May 15, 1964).

5. G. L. Gdalevich, "Measurement of Electrostatic-Field Intensity on the Surface of Rocket During its Flight in the Ionosphere," Iskusst. Sputniki Zemli (USSR), No. 17, 42-58 (1963).

6. Palmer, Jeremy M., "A New Electrostatic Field Measuring Instrument," IEEE Trans. Aerospace, AS-3, Supplement, 523-27 (June 1965).

7. Cole, Robert K., and Sellen, Jr., J. M., "Field Strength Measurements by Emissive E-Meters," AIAA Third Aerospace Sciences Meeting, New York, N. Y., AIAA Paper No. 66-74 (January 14, 1966).

8. O'Brien, Brian J., "The Magnetosphere and Auroras," Astronautics and Aeronautics, (July 1967).

9. Levine, S. H., Harrison, S. R., and Miller, A. C., "Feasibility of Using Radioactive Sources to Measure Electric Field Intensity in Space," NSL 66-160, Contract Report under Contract NAS2-2895, (November 1966).

REFERENCES (CONTINUED)

10. Forrester, A. T., "Analysis of the Ionization of Cesium Ion Tungsten Capillaries," Journ. Chem. Phys., 42, 972 (1965).

11. Bates, T. R., and Forrester, A. T., "Coupled Molecular Flow and Surface Diffusion Application to Cesium Transport," Journ. of Appl. Phys. 38, 1956 (1967).

12. Reynolds, T. W., and Krepo, L. W., NASA Technical Note D-871, (August 1961).

13. Huber, H., and LeBihan, R., "Capillary Cesium Ion Emitter: Application Thermionic Converters," preprint of paper presented at the 13th General Assembly of AGARD, Athens, Greece, (July 10-12, 1963).

14. Krulikovskiy, B. K., "Alkali Metal Source of Ions," Technical Documents Liaison Office, Wright-Patterson Air Force Base, Ohio, AD 649 481, (October 11, 1960).

NASA-Langley, 1968 —— 24 CR-970